



· 论 著 ·

基于高分辨率CT征象建立logistic回归模型对IA期肺腺癌高级别模式的预测价值

董浩¹, 邱勇刚¹, 汪鑫斌¹, 杨俊杰², 楼存诚¹, 叶晓丹^{3,4,5}

1. 杭州市萧山区第一人民医院放射科, 浙江 杭州 311200;
2. 杭州市萧山区第一人民医院病理科, 浙江 杭州 311200;
3. 复旦大学附属中山医院放射科, 上海 200032;
4. 上海医学影像研究所, 上海 200032;
5. 复旦大学附属中山医院肿瘤中心, 上海 200032

[摘要] 背景与目的: 研究表明, 当存在高级别组织学模式(微乳头状和实体模式)时, 肺腺癌患者的预后明显较差, 往往需要更积极的治疗方式, 术前确定浸润性肺腺癌中是否存在任何高级别模式(high-grade pattern, HGP)可以帮助预测患者的预后并确定治疗策略。本研究旨在建立基于高分辨率计算机体层成像(computed tomography, CT)征象的logistic回归模型预测IA期肺腺癌的HGP。方法: 回顾性分析经病理学检查证实为IA期肺腺癌的443例患者(445个病灶)的临床、病理学及影像学资料。根据病理学检查结果有无HGP将445个病灶分成两组: HGP组($n=88$ 个)和非HGP(non-HGP, n-HGP)组($n=357$ 个)。患者的临床病理学资料包括年龄、性别、吸烟史、肿瘤位置、分期及病理生长方式等。CT影像学上观察病灶大小、密度、形状、毛刺征、分叶征、空泡征、空气支气管征、胸膜凹陷征等。两组间定量参数比较采用Mann-Whitney U 检验, 计数资料采用 χ^2 检验或Fisher确切概率法。采用单因素结合多因素logistic回归分析筛选独立预测因子, 并根据多因素logistic回归分析结果分别构建临床模型、CT模型及临床-CT模型, 模型间诊断效能的比较采用DeLong检验。结果: 单因素分析中HGP组与n-HGP组之间年龄、性别、吸烟史、肿瘤大小、密度、形状、毛刺、分叶征、胸膜牵拉差异有统计学意义($P<0.05$), 多因素logistic回归分析结果显示肿瘤大小($P=0.040$; OR=1.063, 95% CI: 1.003~1.126)、密度($P<0.001$; OR=8.249, 95% CI: 4.244~16.034)、分叶征($P=0.001$; OR=3.101, 95% CI: 1.598~6.021)是HGP的独立预测因素, 临床模型、CT模型、临床-CT模型预测HGP的曲线下面积(area under curve, AUC)值分别为0.634、0.838及0.834。结论: 肿瘤大小、密度与分叶征是IA期肺腺癌HGP的独立预测因子。基于高分辨率CT征象的logistic回归模型具有较好的诊断效能, 可以为临床诊断及制订外科治疗方案提供一定的参考依据。

[关键词] 肺腺癌; 高级别模式; 预测模型; 高分辨率CT

中图分类号: R734.2 文献标志码: A DOI: 10.19401/j.cnki.1007-3639.2023.08.005

Predictive value of logistic regression model based on high-resolution CT signs for high-grade pattern in stage I A lung adenocarcinoma DONG Hao¹, QIU Yonggang¹, WANG Xinbin¹, YANG Junjie², LOU Cuncheng¹, YIN Lekang³, YE Xiaodan^{3,4,5} (1. Department of Radiology, First People's Hospital of Xiaoshan District, Hangzhou 311200, Zhejiang Province, China; 2. Department of Pathology, First People's Hospital of Xiaoshan District, Hangzhou 311200, Zhejiang Province, China; 3. Department of Radiology, Zhongshan Hospital, Fudan University, Shanghai 200032, China; 4. Shanghai Institute of Medical Imaging, China; 5. Department of Cancer Center, Zhongshan Hospital, Fudan University, Shanghai 200032, China)

Correspondence to: YE Xiaodan, E-mail: yuanyxd@163.com.

基金项目: 国家自然科学基金(81571629、82071990); 上海市科学技术委员会项目(19411965200); 浙江省医药卫生科技计划项目(2023RC252); 杭州市农业与社会发展科研引导项目(20220919Y078); 杭州市萧山区社会发展重大科技计划政策引导项目(2021309)。

第一作者: 董浩 (ORCID: 0000-0003-3345-5506), 硕士研究生在读。

通信作者: 叶晓丹 (ORCID: 0000-0003-3059-2740), 主任医师, E-mail: yuanyxd@163.com。

[**Abstract**] **Background and purpose:** Studies have shown that when high-grade histological patterns (micropapillary and solid patterns) are present, patients with lung adenocarcinoma have a significantly poorer prognosis and often require more aggressive treatment modalities, and preoperative determination of the presence of any high-grade patterns (HGP) in invasive lung adenocarcinoma can help predict patient prognosis and determine treatment strategies. The aim of the study was to establish a logistic regression model based on high-resolution CT signs to predict the HGP of stage I A lung adenocarcinoma. **Methods:** The clinical, pathological and imaging data of 443 patients (445 lesions) with stage I A lung adenocarcinoma confirmed by pathology diagnosis from First People's Hospital of Xiaoshan District (Oct. 2018 to Mar. 2021) and Zhongshan Hospital of Fudan University (Jan. 2018 to Dec. 2020) were retrospectively analyzed. The 445 lesions were divided into two groups according to the presence or absence of HGP in pathological findings: HGP ($n=88$) and non-HGP (n-HGP) ($n=357$). The clinical and pathological data of the patients included age, gender, smoking history, tumor location, stage and pathological growth pattern. On CT imaging, the size, density, shape, burr sign, lobulation sign, vacuole sign, air bronchus sign and pleural depression sign were observed. Mann-Whitney U test was used to compare quantitative parameters between the two groups, and χ^2 test or Fisher's exact test was used for enumeration of data. The independent predictors were screened by univariate combined with multivariate logistic regression analysis, and the clinical model, CT model and clinical-CT model were constructed according to the results of multivariate logistic regression analysis. DeLong test was used to compare the diagnostic efficacy between models. **Results:** In the univariate analysis, there were significant differences in age, gender, smoking history, tumor size, density, shape, burr, lobulation sign and pleural traction between the HGP group and the n-HGP group ($P<0.05$). Multivariate logistic regression analysis showed tumor size ($P=0.04$; OR=1.063, 95% CI: 1.003-1.126), density ($P<0.001$; OR=8.249, 95% CI: 4.244-16.034), lobulation sign ($P=0.001$; OR=3.101, 95% CI: 1.598-6.021) were independent predictors of HGP, and the area under curve (AUC) values of clinical model, CT model and clinical-CT model for predicting HGP were 0.634, 0.838 and 0.834, respectively. **Conclusion:** Tumor size, density and lobulation sign are independent predictors of HGP in stage I A lung adenocarcinoma. The logistic regression model based on high-resolution CT signs has good diagnostic performance and can provide a certain reference for clinical diagnosis and surgical treatment.

[**Keywords**] Lung adenocarcinoma; High-grade pattern; Prediction model; High-resolution CT

国际肺癌研究协会 (International Association for the Study of Lung Cancer, IASLC)、美国胸腔学会 (The American Thoracic Society, ATS) 和欧洲呼吸学会 (European Respiratory Society, ERS) 的2011年分类系统将肺腺癌分为5种不同的组织学模式: 附壁、腺泡状、乳头状、微乳头状和实体^[1]。多项研究^[2-3]结果表明, 当存在任何高级别组织学模式 (微乳头状和实体模式) 时, 肺腺癌患者的预后明显较差。即使在总体预后较好的 I A 期肺腺癌患者中, 具有高级别模式 (high-grade pattern, HGP) 的患者同样预后不佳^[4]。早期肺腺癌最佳治疗手段通常是根治性切除治疗^[5]。然而, 微乳头或实体模式的存在被认为是术后复发的独立预测因素^[6-7]。具有HGP的早期肺腺癌往往需要更积极的治疗方式^[4, 8]。由于肺腺癌具有很大的异质性, 有时候术中快速冷冻切片病理学检查结果有低估肺腺癌组织学模式的风险^[9]。因此, 在手术前确定浸润性肺腺癌中是否存在任何HGP可以帮助预测患者的预后并确定治疗策略。目前

利用高分辨率计算机断层成像 (high resolution computed tomography, HRCT) 图像预测 I A 期肺腺癌HGP的报道鲜见。本研究基于患者的HRCT图像来预测肺腺癌的高级别模式, 旨在为临床的诊疗工作提供更加准确和有价值的信息, 帮助临床优化治疗方案, 改善患者的预后。

1 资料和方法

1.1 病例资料

回顾性分析2018年10月—2021年3月在复旦大学附属中山医院及2018年1月—2020年12月在杭州市萧山区第一人民医院胸外科接受手术切除且经术后病理学检查结果证实为肺腺癌患者的临床病理学资料及CT诊断等影像学资料。患者纳入标准: ① 手术切除且病理学检查结果证实为肺腺癌; ② 临床TNM分期为T₁N₀M₀期 (I A 期); ③ CT检查前未接受任何放疗或CT引导下穿刺活组织病理学检查。排除标准: ① 浸润前病变、微浸润性腺癌、浸润性腺癌变异型; ② 术

前1个月内未接受HRCT检查;③严重的呼吸运动伪影;④CT图像中可见任何肿大淋巴结的病例。术后病理学检查结果显示,存在多个病灶的患者,每个病灶均作为独立病灶进行分析。患者的临床病理学资料包括年龄、性别、吸烟史、肿瘤位置、肿瘤分期、肿瘤生长方式等。肿瘤分期基于IASLC第8版TNM肺癌分期系统。这项研究得到了参与医院的伦理审查委员会的批准(复旦大学附属中山医院伦理批件号B2021-128,杭州市萧山区第一人民医院伦理批件号2022-XS-076)。

1.2 检查方法

复旦大学附属中山医院采用德国西门子SOMATOM Definition AS+128层螺旋CT机及荷兰飞利浦Brilliance 64层螺旋CT机进行扫描,杭州市萧山区第一人民医院应用飞利浦Brilliance 64层螺旋机进行扫描。西门子CT机扫描参数:管电压120 KV,管电流250 mA,螺距1.1。飞利浦CT机扫描参数:管电压130 KV,管电流200 mA,螺距0.64。所有患者扫描前均进行屏气训练,扫描时平静呼吸下屏气,扫描范围从肺尖到肺底,两侧包括腋窝和胸壁。CT扫描均为平扫CT检查。重建算法为高分辨率算法(西门子CT, BF=70;飞利浦CT,肺算法),重建层厚1 mm,重建间隔1 mm。

1.3 图像分析

由一位拥有10年及一位拥有20年胸部CT影像学诊断经验的放射科医师,在事先不知道病理学检查结果的情况下各自对CT图像进行独立回顾性分析,意见不一致时,商讨后取得一致意见。CT影像学上对病灶描述包括肿瘤大小、密度、形状、毛刺征、分叶征、空泡征、空气支气管征、胸膜凹陷征。肿瘤大小定义为三维图像上最大横截面的长径,密度按是否含有磨玻璃影分为实性结节(solid nodule, SN)及亚实性结节(subsolid nodule, SSN)。

1.4 病理学检查及分组

病理学检查的标本常规固定在4%的甲醛溶液中,然后石蜡包埋。将包括肿瘤最大切面的组织切成厚度为4 μm 的切片,并采用H-E染色。

由一名经验丰富的病理科医师根据最新的侵袭性肺腺癌分级系统^[10]进行病理学诊断。对于每个病例,以半定量(总和为100%)的方式对原发肿瘤进行组织学模式划分,当任何一种含量超过1%时即定义为含有该模式。根据病理学检查结果有无HGP将445个病灶分成两组:HGP组和非HGP(non-HGP, n-HGP)组。

1.5 统计学处理

采用Shapiro-Wilk检验对计量资料进行正态检验,符合正态分布的计量资料以 $\bar{x} \pm s$ 表示,并采用 t 检验。计数资料两组间比较采用 χ^2 检验或Fisher确切概率法。采用单因素结合多因素logistic回归分析筛选HGP的独立预测因子,并计算出相应的比值比(odds ratio, OR)。根据多因素logistic回归分析结果分别构建临床模型、CT模型及临床-CT模型。采用logistic回归分析时,将n-HGP、HGP作为因变量(n-HGP=0, HGP=1),将单因素差异有统计学意义的临床和CT特征作为自变量。CT特征的观察者之间一致性通过组内相关系数(intra-class correlation, ICC)及Kappa值进行评估。对具有统计学意义的单因素参数及logistic回归模型预测概率进行受试者工作特征(receiver operating characteristic, ROC)曲线分析,得出曲线下面积(area under curve, AUC)、灵敏度、特异度,比较模型间诊断效能采用DeLong检验。采用Hosmer-Lemeshow拟合优度检验评价模型,如 $P > 0.05$ 为可接受的水平上模型的估计拟合了数据,表明评分模型工作效果良好。 $P < 0.05$ 为差异有统计学意义。使用R软件(4.2.3版本, <http://www.r-project.org>)进行统计学分析和统计作图。

2 结果

2.1 HGP组与n-HGP组病灶的临床与病理学资料

最终纳入复旦大学附属中山医院(357例)及杭州市萧山区第一人民医院(86例)共计443例患者的445个病灶,其中单发病灶441例,双发病灶2例,双发病灶均来自同一肺叶。男性157例、女性

286例, 年龄25~87 (58±11) 岁。本研究结果显示, HGP组与n-HGP组在年龄、性别、吸烟史、临床T分期上差异均有统计学意义 ($P=0.037$ 、 $P=0.015$ 、 $P=0.003$ 和 $P<0.001$)。病理学上HGP组全部以混合形式出现。两组比较差异有统计学意义 ($P=0.008$), 两组的主要组织学模式差异有统计学意义 ($P<0.001$)。两组的肿瘤位置差异无统计学意义 ($P=0.401$, 表1)。

2.2 CT 特征的观察者间一致性

肿瘤大小的ICC值为0.997 (95% CI:

0.997~0.998), 其他CT特征的Kappa值为0.791~0.986 (表2)。结果表明, CT特征的观察者间一致性较好。

2.3 HGP组与n-HGP组病灶与CT特征的相关性

本研究结果显示, HGP组平均肿瘤直径大于n-HGP组 ($P<0.001$), HGP组出现SN、不规则形状、毛刺、分叶以及胸膜牵拉的频率明显高于n-HGP组 ($P<0.001$ 、 $P=0.003$ 、 $P<0.001$ 、 $P<0.001$ 和 $P<0.001$)。空泡征及空气支气管征差异无统计学意义 ($P=0.764$ 、 $P=0.162$, 表3)。

表1 患者的临床病理学特征

Tab. 1 Clinical and pathological characteristics of patients

| Item | Total | HGP (n=88) | n-HGP (n=357) | P value |
|-----------------------------|-------|------------|---------------|---------------------|
| Age/year | 58±11 | 57±12 | 61±9 | 0.037 [△] |
| Gender | | | | 0.015 [#] |
| Male | 158 | 41 | 117 | |
| Female | 287 | 47 | 240 | |
| Smoking history | | | | 0.003 [#] |
| No | 390 | 69 | 321 | |
| Yes | 55 | 19 | 36 | |
| Location | | | | 0.401 [#] |
| Left upper lobe | 108 | 22 | 86 | |
| Left lower lobe | 69 | 17 | 52 | |
| Right upper lobe | 148 | 29 | 119 | |
| Right middle lobe | 36 | 9 | 27 | |
| Right lower lobe | 84 | 11 | 73 | |
| Clinical T staging | | | | <0.001 [#] |
| T _{1a} | 121 | 10 | 111 | |
| T _{1b} | 258 | 54 | 204 | |
| T _{1c} | 66 | 24 | 42 | |
| Pure or mix pattern | | | | 0.008 [*] |
| Pure | 27 | 0 | 27 | |
| Mix | 418 | 88 | 330 | |
| Major histological patterns | | | | <0.001 [*] |
| Lepidic predominant | 52 | 1 | 51 | |
| Acinar predominant | 348 | 71 | 280 | |
| Papillary predominant | 32 | 6 | 26 | |
| Micropapillary | 4 | 4 | 0 | |
| Solid predominant | 9 | 9 | 0 | |

△: t-test, #: Chi-square test; *: Fisher's exact test.

表2 CT特征的观察者一致性检验结果

Tab. 2 Observer consistency test results for CT features

| Item | Case <i>n</i> | SE | Kappa value | 95% CI |
|---------------------|---------------|-------|-------------|-------------|
| Density | 443 | 0.012 | 0.983 | 0.955-1.000 |
| Shape | 440 | 0.013 | 0.972 | 0.942-0.994 |
| Lobulation | 422 | 0.022 | 0.892 | 0.847-0.933 |
| Spiculation | 430 | 0.018 | 0.924 | 0.886-0.956 |
| Vacuole | 427 | 0.048 | 0.791 | 0.685-0.837 |
| Air bronchogram | 435 | 0.015 | 0.955 | 0.926-0.982 |
| Pleural indentation | 442 | 0.008 | 0.986 | 0.968-1.000 |

SE: Standard error.

表3 HGP组与n-HGP组病灶CT特征比较

Tab. 3 Comparison of CT features of lesions between the HGP and n-HGP groups

| Item | Total | HGP (<i>n</i> =88) | n-HGP (<i>n</i> =357) | <i>P</i> value |
|-------------------------|-------|---------------------|------------------------|---------------------|
| Tumor size <i>D</i> /mm | 14±5 | 17±5 | 14±5 | <0.001 [△] |
| Density | | | | <0.001 [#] |
| SSN | 377 | 45 | 332 | |
| SN | 68 | 43 | 25 | |
| Shape | | | | 0.003 [#] |
| Round or oval | 129 | 14 | 115 | |
| Irregular | 316 | 74 | 242 | |
| Lobulation | | | | <0.001 [#] |
| No | 287 | 25 | 262 | |
| Yes | 158 | 63 | 95 | |
| Spiculation | | | | <0.001 [#] |
| No | 296 | 32 | 264 | |
| Yes | 149 | 56 | 93 | |
| Vacuole | | | | 0.764 [#] |
| No | 406 | 81 | 325 | |
| Yes | 39 | 7 | 32 | |
| Air bronchogram | | | | 0.162 [#] |
| No | 242 | 42 | 200 | |
| Yes | 203 | 46 | 157 | |
| Pleural indentation | | | | <0.001 [#] |
| No | 256 | 33 | 223 | |
| Yes | 189 | 55 | 134 | |

[△]: *t*-test, [#]: Chi-square test.

2.4 临床指标及CT特征的多因素回归分析

对单因素分析中具有统计学意义的临床指标及CT特征进行多因素logistic回归分析，纳入因素包括患者年龄、性别、吸烟史、肿瘤大小、密度、形状、毛刺、分叶征、胸膜牵拉。多因素logistic回归分析结果显示，

肿瘤大小 ($P=0.04$; $OR=1.063$, 95% $CI: 1.003\sim 1.126$)、密度 ($P<0.001$; $OR=8.249$, 95% $CI: 4.244\sim 16.034$)、分叶征 ($P=0.001$; $OR=3.101$, 95% $CI: 1.598\sim 6.021$) 是预测HGP的独立预测因子 (图1、2)。

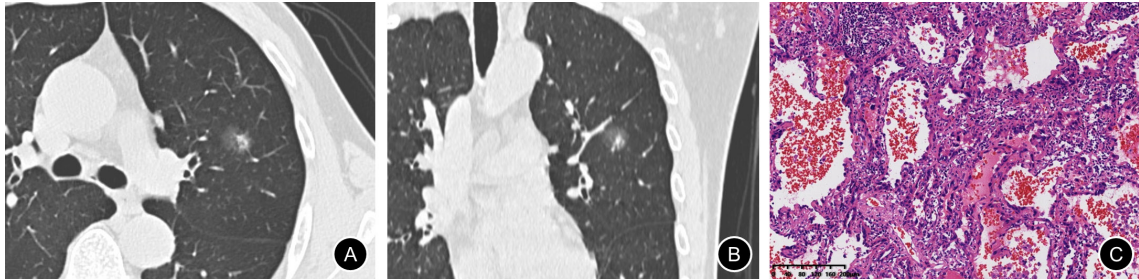


图1 左肺上叶SSN的影像学及病理学诊断结果

Fig. 1 CT and pathology images of SSN in the upper lobe of the left lung

A 55-year-old male patient, no smoking history. A: HRCT transection lung window showed SSN in the upper lobe of the left lung, with a length diameter of about 15 mm and no lobes around it; B: Reconstructed image (coronal position), nodules did not show lobulation signs; C: Pathological diagram, the result was acinar predominant invasive adenocarcinoma (H-E, $\times 100$).



图2 右肺下叶SN的影像学及病理学诊断结果

Fig. 2 CT and pathology images of SN in the lower lobe of the right lung

A 58-year-old male patient with a smoking history of 30 years. A: HRCT transection lung window showed SN in the upper lobe of the left lung, with a long diameter of about 26 mm, and the lobulation sign was visible around the periphery; B: Reconstruction image (coronal position), nodules showed lobulation signs; C: Pathological diagram, the result was solid predominant invasive adenocarcinoma (H-E, $\times 100$).

2.5 回归模型的构建与比较

根据多因素logistic回归分析结果构建3个模型：临床模型、CT特征模型和临床-CT模型。ROC曲线分析得出的AUC值分别为0.634、0.838及0.834 (图3)。DeLong检验显示，CT模型及临床-CT模型均优于单独使用临床变量来预测HGP ($P<0.001$ 、 $P<0.001$)，CT模型AUC略高于临床-CT模型，但两者差异无统计学意义 ($P=0.570$)，灵敏度为70.5%，特异度为84.9%。CT模型诊断效能优于各单因素CT征象 (表4)。CT模型Hosmer-Lemeshow检验结果表明模型拟合度良好 ($P=0.295$)。

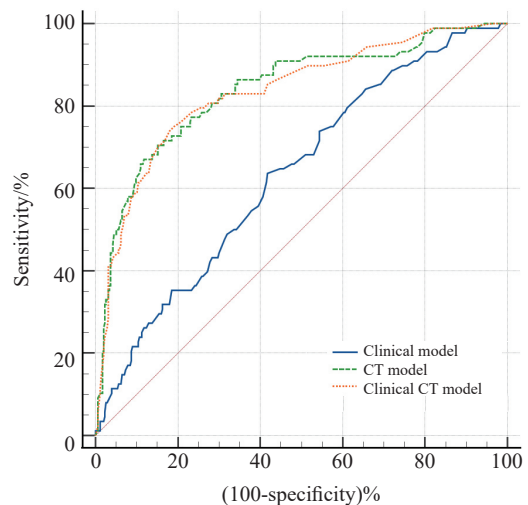


图3 临床模型、CT模型及临床-CT模型预测HGP的ROC曲线

Fig. 3 ROC curves predicted by clinical model, CT model and clinical-CT model

表4 CT模型及各单因素征象预测HGP的诊断效能比较

Tab. 4 Comparison of diagnostic performance of CT model and univariate signs in predicting HGP

| Item | AUC (95% CI) | Sensitivity/% | Specificity/% |
|---------------------|---------------------|---------------|---------------|
| CT model | 0.838 (0.788-0.889) | 70.5 | 84.9 |
| Tumor size | 0.695 (0.636-0.755) | 75.0 | 56.4 |
| Density | 0.709 (0.640-0.778) | 48.9 | 97.0 |
| Shape | 0.582 (0.519-0.644) | 84.1 | 32.2 |
| Lobulation | 0.725 (0.664-0.785) | 71.6 | 73.4 |
| Spiculation | 0.688 (0.624-0.752) | 63.6 | 73.9 |
| Pleural indentation | 0.625 (0.560-0.690) | 62.5 | 62.5 |

3 讨 论

晚期肺癌死亡率高^[11],严重影响人类健康。腺癌是最常见的肺癌组织学类型,几乎占有肺癌的一半^[12]。研究^[13-15]证实,CT征象能较好地区分浸润性肺腺癌与浸润前病变/微浸润性腺癌,但CT特征在浸润性肺腺癌各组织学模式之间的差异很少有报道。近年来有研究^[16]表明,肺内淋巴结转移在临床分期 IA 肺腺癌中很常见。腺癌组织学模式是影响早期肺癌淋巴结转移的重要因素,实体或微乳头为主的患者有明显更多的淋巴结转移^[17]。因此,利用CT特征鉴别出具有HGP的肺腺癌具有重要意义,可以为临床预测肿瘤进展和决定诊治方案提供重要信息^[18]。

本研究表明,有吸烟史的中老年男性更有可能出现HGP。Jeon等^[4]发现,吸烟史与 IA 期肺腺癌的生存率相关($P=0.04$)。本研究结果显示,男性患者更有可能出现HGP,这可能与男性患者吸烟比例较高有关。本研究病理学诊断结果显示,绝大多数肺腺癌的组织学模式都是混合性,单纯性生长仅占一小部分(5.9%),有研究^[19]结果显示,只有6%~22%的浸润性腺癌是由单一组织学模式组成的纯病理学模式,与本研究结果基本一致。本研究结果显示,含HGP的 IA 期肺腺癌全部以混合形式出现,并且无论是HGP组与n-HGP组,主要生长模式多为腺泡型(77.7% vs 80.2%),与Choi等^[8]的研究结果基本一致。

本研究中多因素logistic回归结果显示,肿瘤

长径是预测具有HGP肺腺癌的独立预测因子。一些研究^[20-21]结果也表明,含有HGP的肿瘤相对更大,可能是因为含HGP的肿瘤生长速度更快导致的,或者我们推测还有另一种可能性,即肿瘤生长的过程中逐步形成了HGP,当然这还需要更多的病理学研究去证实。IA期肺腺癌中实体模式比例较高者往往预后更差^[22],本研究结果显示,HGP表现为SN的比例更高。有研究^[23]结果显示,在 IA 期肺腺癌患者中,病灶表现为SN是独立的预后因素。另有研究^[24]结果显示,表现为SN的 IA 期肺腺癌的男性患者预后不良,与本研究结果不尽相同。本研究结果证实,分叶征是预测HGP的独立预测因子,分叶征的病理学基础可能是肿瘤边缘部位生长速度不同或肺泡间隔、小叶间隔的阻挡引起肿瘤生长受限而形成分叶。总之,本研究结果提示,直径较大的、表现为分叶征的SN更可能出现HGP。

本研究有如下局限性:首先,作为一项回顾性研究,可能存在不可避免的选择偏倚;其次,不同CT扫描仪扫描出的图像可能对结果产生一定的影响;再次,缺乏定量参数评价,例如密度值、体积等。后续我们将联合多中心、扩大样本量并加入定量参数继续进行研究。

综上所述, IA 期肺腺癌的高分辨率CT征象与其是否含有HGP有一定的相关性,肿瘤大小、密度与分叶征是预测HGP的独立预测因子。本研究结果表明,基于HRCT征象的logistic回归模型具有较好的诊断效能,可以为临床诊治提供依据,帮助改善患者的预后。

利益冲突声明：所有作者均声明不存在利益冲突。

[参 考 文 献]

- [1] TRAVIS W D, BRAMBILLA E, NOGUCHI M, et al. International Association for the Study of Lung Cancer/American Thoracic Society/European Respiratory Society international multidisciplinary classification of lung adenocarcinoma [J]. *J Thorac Oncol*, 2011, 6(2): 244–285.
- [2] TAKAHASHI Y, EGUCHI T, KAMEDA K, et al. Histologic subtyping in pathologic stage I–II A lung adenocarcinoma provides risk-based stratification for surveillance [J]. *Oncotarget*, 2018, 9(87): 35742–35751.
- [3] YASUKAWA M, OHBAYASHI C, KAWAGUCHI T, et al. Analysis of histological grade in resected lung-invasive adenocarcinoma [J]. *Anticancer Res*, 2019, 39(3): 1491–1500.
- [4] JEON H W, KIM Y D, SIM S B, et al. Significant difference in recurrence according to the proportion of high grade patterns in stage I A lung adenocarcinoma [J]. *Thorac Cancer*, 2021, 12(13): 1952–1958.
- [5] VAN SCHIL P E, ASAMURA H, RUSCH V W, et al. Surgical implications of the new IASLC/ATS/ERS adenocarcinoma classification [J]. *Eur Respir J*, 2012, 39(2): 478–486.
- [6] HUNG J J, JENG W J, CHOU T Y, et al. Prognostic value of the new International Association for the Study of Lung Cancer/American Thoracic Society/European Respiratory Society lung adenocarcinoma classification on death and recurrence in completely resected stage I lung adenocarcinoma [J]. *Ann Surg*, 2013, 258(6): 1079–1086.
- [7] HUNG J J, YEH Y C, JENG W J, et al. Predictive value of the International Association for the Study of Lung Cancer/American Thoracic Society/European Respiratory Society classification of lung adenocarcinoma in tumor recurrence and patient survival [J]. *J Clin Oncol*, 2014, 32(22): 2357–2364.
- [8] CHOI Y, KIM J, PARK H, et al. Rethinking a non-predominant pattern in invasive lung adenocarcinoma: prognostic dissection focusing on a high-grade pattern [J]. *Cancers (Basel)*, 2021, 13(11): 2785.
- [9] TAKAHASHI Y, KURODA H, OYA Y, et al. Challenges for real-time intraoperative diagnosis of high risk histology in lung adenocarcinoma: a necessity for sublobar resection [J]. *Thorac Cancer*, 2019, 10(8): 1663–1668.
- [10] ANDRE L, MOREIRA, MD P, et al. A grading system for invasive pulmonary adenocarcinoma: a proposal from the international association for the study of lung cancer pathology committee [J]. *J Thorac Oncol*, 2020, 15(10): 1599–1610.
- [11] SUNG H, FERLAY J, SIEGEL R L, et al. Global cancer statistics 2020: GLOBOCAN estimates of incidence and mortality worldwide for 36 cancers in 185 countries [J]. *CA Cancer J Clin*, 2021, 71(3): 209–249.
- [12] KUHN E, MORBINI P, CANCELLIERI A, et al. Adenocarcinoma classification: patterns and prognosis [J]. *Pathologica*, 2018, 110(1): 5–11.
- [13] ZHANG Y, QIANG J W, SHEN Y, et al. Using air bronchograms on multi-detector CT to predict the invasiveness of small lung adenocarcinoma [J]. *Eur J Radiol*, 2016, 85(3): 571–577.
- [14] 金鑫, 赵绍宏, 高洁, 等. 纯磨玻璃密度肺腺癌病理分类及影像表现特点分析 [J]. *中华放射学杂志*, 2014, 48(4): 283–287
- JIN X, ZHAO S H, GAO J, et al. Pathological classification and imaging characteristics of early-stage lung adenocarcinoma with pure ground-glass opacity [J]. *Chin J Radiol*, 2014, 48(4): 283–287
- [15] 蔡蒙婷, 纪晓微, 傅钢泽, 等. 含气腔型浸润性肺小腺癌的CT表现与病理分型的对照研究 [J]. *中华放射学杂志*, 2019, 53(10): 886–891.
- [16] ZHANG D G, CHEN X C, ZHU D X, et al. Intrapulmonary lymph node metastasis is common in clinically staged I A adenocarcinoma of the lung [J]. *Thorac Cancer*, 2019, 10(2): 123–127.
- [17] YU Y, JIAN H, SHEN L, et al. Lymph node involvement influenced by lung adenocarcinoma subtypes in tumor size ≤ 3 cm disease: a study of 2 268 cases [J]. *Eur J Surg Oncol*, 2016, 42(11): 1714–1719.
- [18] MIKUBO M, NAITO M, MATSUI Y, et al. Relevance of intraoperative pleural lavage cytology and histologic subtype in lung adenocarcinoma [J]. *Ann Thorac Surg*, 2018, 106(6): 1654–1660.
- [19] LEE G, CHOI E R, LEE H Y, et al. Pathologic heterogeneity of lung adenocarcinomas: a novel pathologic index predicts survival [J]. *Oncotarget*, 2016, 7(43): 70353–70363.
- [20] SUNG Y E, LEE K Y, MOON Y. The prognostic utility of the histologic subtype of stage I lung adenocarcinoma may be diminished when using only the invasive component to determine tumor size for tumor node metastasis (TNM) staging [J]. *J Thorac Dis*, 2021, 13(5): 2910–2922.
- [21] CHEN L W, YANG S M, WANG H J, et al. Prediction of micropapillary and solid pattern in lung adenocarcinoma using radiomic values extracted from near-pure histopathological subtypes [J]. *Eur Radiol*, 2021, 31(7): 5127–5138.
- [22] SUN F H, HUANG Y W, YANG X D, et al. Solid component ratio influences prognosis of GGO-featured I A stage invasive lung adenocarcinoma [J]. *Cancer Imaging*, 2020, 20(1): 87.
- [23] MIYOSHI T, AOKAGE K, KATSUMATA S, et al. Ground-glass opacity is a strong prognosticator for pathologic stage I A lung adenocarcinoma [J]. *Ann Thorac Surg*, 2019, 108(1): 249–255.
- [24] MA X, ZHOU S, HUANG L, et al. Assessment of relationships among clinicopathological characteristics, morphological computer tomography features, and tumor cell proliferation in stage I lung adenocarcinoma [J]. *J Thorac Dis*, 2021, 13(5): 2844–2857.

(收稿日期: 2023-02-03 修回日期: 2023-05-12)